Finite difference time domain study of high efficiency photonic crystal superprisms

Toshihiko Baba, Takashi Matsumoto and Manabu Echizen

Yokohama National University, Department of Electrical and Computer Engineering
79-5 Tokiwadai, Hodogayaku, Yokohama 240-8501, Japan
baba@ynu.ac.jp

Abstract: Input and output boundaries of a photonic crystal (PC) are optimized so that the superprism exhibits low insertion loss. It is shown that projected-airhole and half-circular airhole interfaces achieve transmission loss of 0.3 dB and 1.0 dB, respectively, for small and large incident angles of light against normal to boundaries. The finite-difference time-domain simulation shows that a low loss is essentially realized by a periodic phase modulation of the incident beam by the interfaces. It also demonstrates the clear steering of collimated light beam with varying wavelength. The enhancement of angular dispersion is also demonstrated by a PC composed of a dispersive medium.

OCIS codes: (230.3990) Microstructure devices; (230.3120) Integrated Optics Device

References and links

1. H. Kosaka, T. Kawashima, A. Tomita, M. Notomi, T. Tamamura, T. Sato, and S. Kawakami, "Superprism phenomena in photonic crystals: toward microscale lightwave circuits," J. Lightwave Technol. **17**, 2032-2034 (1999).
2. T. Baba and M. Nakamura, "Photonic crystal light deflection devices using the superprism effect," IEEE J. Quantum Electron. **38**, 909-914 (2002).
3. L. J. Wu, M. Mazilu, T. Karle, and T. F. Krauss, "Superprism phenomena in planar photonic crystals," IEEE J. Quantum Electron. **38**, 915-918 (2002).
4. K. B. Chung, and S. W. Hong, "Wavelength demultiplexers based on the superprism phenomena in photonic crystals," Appl. Phys. Lett. **81**, 1549-1551 (2002).
5. T. Prasad, V. Colvin, and D. Mittleman, "Superprism phenomenon in three-dimensional macroporous polymer photonic crystals," Phys. Rev. B **67**, 165103-165109 (2003)
6. D. Scrymgeour, N. Malkova, S. Kim, and V. Gopalan, "Electro-optic control of the superprism effect in photonic crystals," Appl. Phys. Lett. 82, 3176-3178 (2003).
7. T. Baba and T. Matsumoto, "Resolution of photonic crystal superprism," Appl. Phys. Lett. **81**, 2325-2327 (2002).
8. T. Matsumoto and T. Baba, "Photonic crystal ***k***-vector superprism," J. Lightwave Technol. **22**, 917-922 (2004).
9. T. Matsumoto and T. Baba, "Design and FDTD simulation of photonic crystal ***k***-vector superprism," IEICE Trans. Electron. **E87-C**, 393-397 (2004).
10. T. Baba and D. Ohsaki, "Interfaces of photonic crystals for high efficiency light transmission," Jpn. J. Appl. Phys. **40**, 5920-5924 (2001).
11. J. Ushida, M. Tokushima, M. Shirane, A. Gomyo, and H. Yamada, "Immittance matching for multidimensional open-system photonic crystals," Phys. Rev. B **68**, 155115-155121 (2003).
12. Y. Suematsu, Ed., Semiconductor Lasers and Integrated Optics, Ohmsha, Tokyo, (1984).

The superprism is a diffraction device of defect-free bulk photonic crystals (PCs), which operates at frequencies of higher order photonic bands [1] It exhibits wide steering of Poynting vector ***S*** in PCs by a small change of frequency and incident angle. Therefore, we call it the ***S***-vector superprism. In early studies, large angular dispersion of this prism arising from an anomalous dispersion characteristic of PCs was focused, and the realization of high performance demultiplexer, beam scanner, and so on, was expected [1-6]. However, the anomalous characteristic simultaneously degrades the quality of light beam, so rather reduces the spatial and spectral resolution [7]. In recent studies, we proposed the ***k***-vector superprism [8,9] which utilizes the steering of ***k*** vector instead of ***S*** vector. The dispersion analysis showed that the ***k***-vector prism improves the resolution by the refraction of highly collimated beam at an angled output end of the PC. In addition, it allows narrow input beam and a compact PC. This point is important not only for the device itself but also for succeeding researches, since it enables us to use more simply the finite-difference time-domain (FDTD) simulation, which is a powerful tool for the design of structural details. Now therefore, the next issue is to find low loss design. Let us consider a standard PC composed of high index contrast media, e.g. airholes in a semiconductor slab (PC slab). Then, the transmittance through the superprism is no higher than 10% due to two reasons. One is a reflection loss at input and output ends caused by a field mismatch between an incident wave and a Bloch wave in the PC. The other is many diffraction beams generated at these ends. Because of these reasons, no studies have succeeded in clear demonstration of the beam steering even in numerical simulations. Some studies theoretically discussed the modification of interfaces to improve the transmittance against the normal incidence of light [2,10,11]. We proposed a projected airhole interface, which smoothly modulates the phase of the incident wave to compensate the field mismatch and theoretically achieves < 0.3 dB total insertion loss [10]. We also showed that diffraction beams are suppressed to some extent by a flat interface [2]. In this paper, we show in the FDTD simulation that the optimization of these interfaces allows clear steering of highly collimated beam with low insertion loss. We also discuss the enhancement of beam steering angle with the help of material dispersion.

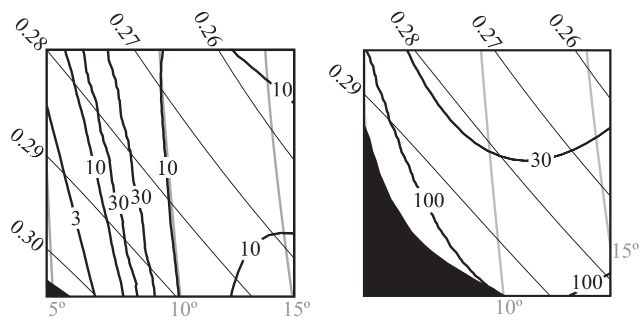

(a) (b)

Fig. 1 Contour plots of eigen frequency (thin black curve), incident angle (thick gray curve) and resolution parameter (thick black curve) of 2D PC in a triangular lattice rotated by 45°. (a) ***S***-vector prism. Resolution parameter of > 30 is omitted. (b) ***k***-vector prism with 45° output end. Black region indicates air lightcone when the structure is airbridge PC slab.

This paper assumes a finite-size two-dimensional (2D) PC composed of airholes in a square lattice rotated by 45° against an input end of the PC. The airhole diameter to lattice constant ratio $2r/a$ is 0.61. The background index is initially fixed to 3.065, which corresponds to an effective modal index of a semiconductor slab [7]. The PC has an output end of 0° or 45° against the input end, and is surrounded by the same background medium. The polarization is assumed to be inside the 2D plane. Figure 1 shows contour plots of eigen frequency, incident angle of light and resolution parameter (an index of resolution). The resolution parameter is defined as $[\partial\theta/\partial(a/\lambda)]/[\partial\theta/\partial\theta_{in}]$, [7,8] where θ is the light propagation angle in the PC and outside of the PC for the ***S***-vector and ***k***-vector prisms, respectively, and θ_{in} is the incident angle. They were calculated by the plane wave expansion method for the second band and plotted in the limited region of the Brillouin zone. Here, the ***k***-vector conservation law was applied for the first and the second Brillouin zones at input and output ends, respectively, assuming the rear side light output. We omit to explain the detail of

Received 5 August 2004; revised 11 September 2004; accepted 14 September 2004

the superprisms, the analysis, and the resolution parameter, because their details are fully explained in Refs. [7-9]. Figure 1 simply indicates an important point for this study, i.e., the best θ_{in} is 10° for the ***k***-vector prism. As shown in this figure, a high resolution parameter of > 30, which is 6 times larger than a typical value of a first order diffraction grating, is obtained as a ***k***-vector prism, when θ_{in} of a Gaussian beam is 10° against normal to the input end and $1/e^2$ full angular divergence of the Gaussian beam is within several degrees. Although the best θ_{in} for the ***S***-vector prism is 7°, a standard resolution parameter as a grating is maintained at 10°. Therefore, θ_{in} is fixed to 10° in this paper.

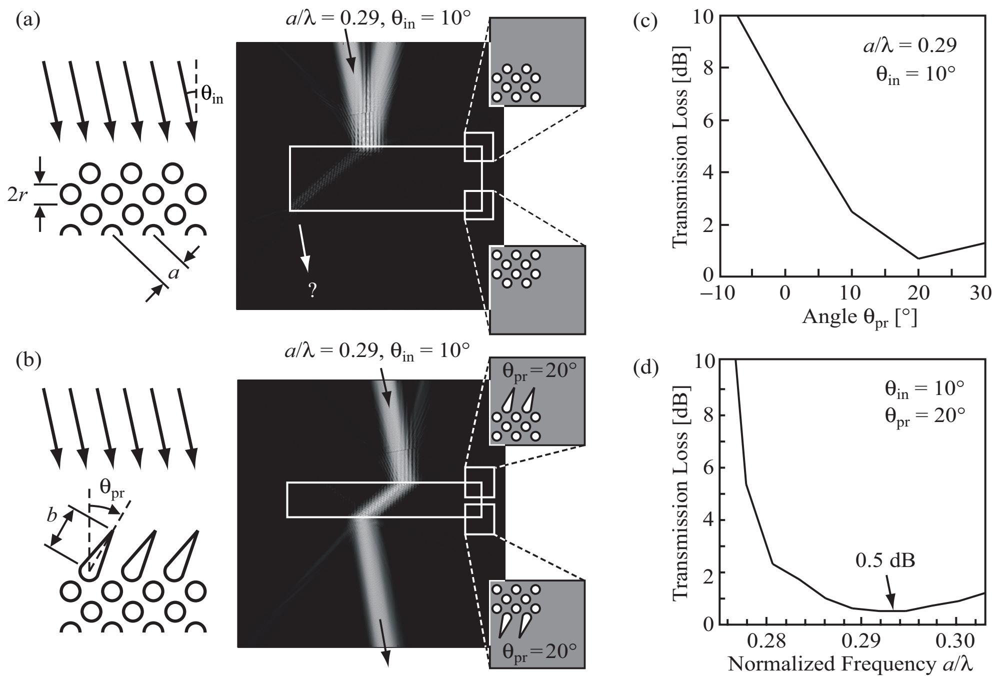

Fig. 2 Light transmission characteristics of ***S***-vector prism. (a) Light intensity distribution for PC without special interfaces. (b) That with projected airhole interfaces. (c) Dependence of insertion loss on angle of projections. (d) Dependence on normalized frequency a/λ.

Figure 2(a) shows the light intensity distribution obtained by the FDTD simulation, when input and output ends have no special interfaces and the Gaussian beam is excited outside of the PC. The $1/e^2$ width of the beam is fixed to 20*a*, which satisfies the above angular divergence condition. At the input end, light is reflected almost perfectly, and very weak intensity enters the PC, exhibiting the negative refraction of the ***S***-vector prism. Due to additional reflection at the 0° output end, light output is hardly observed. In many calculations, we noticed that the result is strongly dependent on θ_{in}. For example, for θ_{in} = 25°, the insertion loss decreases up to 2.4 dB. However, light exhibits the positive refraction in the PC, which is not the operation expected as an ***S***-vector prism. This implies that the interface must be optimized individually for the target incident angle and Bloch wave. In principle, however, the interface should act as a phase modulator which compensates the field mismatch. Based on this concept, we considered a projected airhole interface for θ_{in} = 10°, as shown in Fig. 2(b). Here, projections are oriented in the opposite direction against the incident beam, i.e. θ_{pr} = 20°, and their length *b* is set to be 1.97*a*. These are critical conditions under which the incident beam uniformly suffers the phase shift from each projection without duplication. Figure 3 shows magnified field profiles at input interfaces with different θ_{pr}. It is clearly observed that the optimum θ_{pr} gives an adequate modulation to the phase front so that

#4988 - $15.00 US Received 5 August 2004; revised 11 September 2004; accepted 14 September 2004

the internal light is smoothly excited. Consequently, the insertion loss is drastically reduced and the clear negative refraction is observed. The lowest loss is 0.5 dB (0.25 dB/interface) when θ_{pr} = 20°, as shown in Fig. 2(c). This loss value is attractive even when the prism is considered as a simple diffraction grating. A loss of < 1 dB is maintained for b/a = 1.8 – 2.3 and in a wide spectral range of a/λ = 0.286 – 0.301, as shown in Fig. 2(d). Figure 4(a) demonstrates the beam steering of the ***S***-vector prism with the optimized interface. The beam divergence at a/λ = 0.275 is caused by a small bend of the frequency contour. Except for this, clear steering of the collimated beam is observed. In the range of a/λ = 0.272 – 0.299, the beam steering angle $\Delta\theta_c$ is 16°, as shown by the solid line in Fig. 4(b). This value almost agrees with that expected from the wavelength sensitivity parameter $\partial\theta_c / \partial(a/\lambda)$ in the dispersion analysis [7].

As a ***k***-vector prism, a structure and light output are considered, as illustrated in Fig. 5(a). A 45° output end is placed on the rear side of the PC so that the internal light dominated by the ***S***-vector prism reaches to this end. The FDTD simulation previously showed that light output occurs in a direction determined by the second Brillouin zone [9]. Such an arrangement of the output end and a direction of light output correspond to assumptions for Fig. 1. The output end is largely inclined against the internal light, so the output beam is expanded to 75a – 150a in width and well collimated. However, the large inclination severely restricts the optimization of the interface. For example, the total insertion loss cannot be lower than 6 dB by the projected airholes, since projections cannot be freely optimized without overlapping. Through trial calculations of many interfaces, we found that half airholes oriented by 60° against normal to the output end gives a low insertion loss of 1.3 dB (~1 dB at the output end). A < 1.5 dB loss is maintained for a/λ = 0.279 – 0.289, and the steering of the collimated beam is observed outside of the PC, as shown in Fig. 5(a). The beam steering angle θ_{out} is smaller than that of the ***S***-vector prism, and is comparable to that of the first order grating. However, the expansion of the output beam improves the beam collimation and realizes the higher resolution.

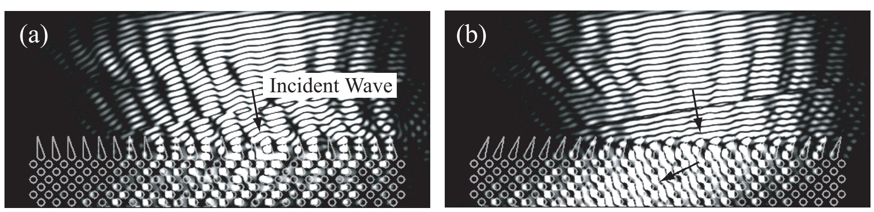

Fig. 3 Shaded drawings of field intensity distribution (**H** field in the direction perpendicular to the 2D plane) of light propagation at input interfaces of PCs. Dark lines denote the shape of airholes. (a) θ_{pr} = –20°. (b) θ_{pr} = 20°.

#4988 - $15.00 US Received 5 August 2004; revised 11 September 2004; accepted 14 September 2004

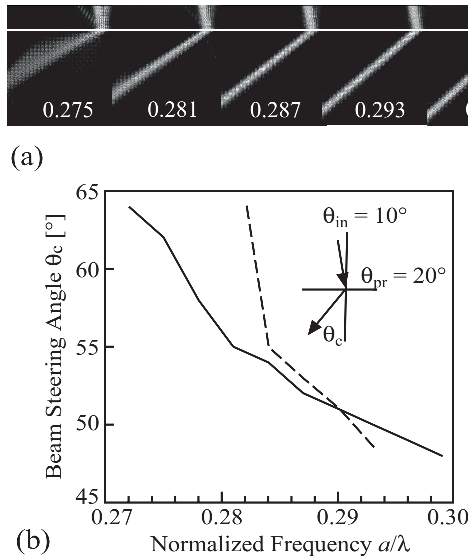

Fig. 4 Beam steering characteristics of ***S***-vector prism. (a) Light intensity distributions for various a/λ. (b) Beam steering angle as a function of a/λ. Solid and dashed lines denote background material of PC without and with material dispersion.

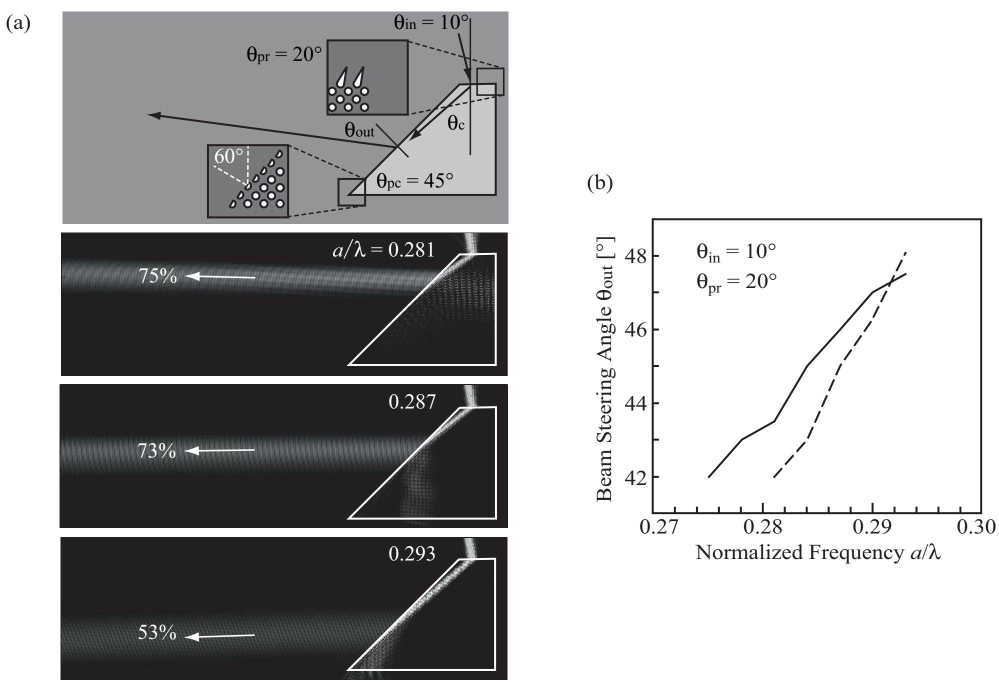

Fig. 5 Beam steering characteristics of ***k***-vector prism. (a) Calculation model and light intensity distributions for various a/λ. (b) Beam steering angle as a function of a/λ. Solid and dashed lines denote background material of PC without and with material dispersion.

To realize a compact demultiplexer by the superprisms, not only the high beam collimation but also the wide beam steering is necessary. The beam steering angle can be enhanced by the material dispersion near the electronic band-edge of the background medium of the PC. Let us consider 1.5-μm-GaInAsP bulk crystal lattice-matched to InP, as an example. Its refractive index is calculated almost precisely to be 3.676 – 3.565 at λ = 1.503 – 1.581, respectively [12]. If an airbridge PC slab of 0.23 μm thickness is assumed, the modal effective index changes in the range of 3.079 – 2.924, respectively. Beam steering angles θ_c and θ_{out} for this material dispersion and a = 0.52 μm are shown by dashed lines in Figs. 4(b) and 5(b). The angles increase to 1.2 – 1.5 times as large as the case of the fixed refractive index. This enhancement is an advantage of superprisms, which cannot be obtained in reflection-type gratings.

In conclusion, projected airhole and half airhole interfaces were assumed, respectively, at input and output ends of a square lattice 2D PC, and the steering of collimated light beam by superprisms was successfully demonstrated in the FDTD simulation. Practical low insertion loss of 0.5 dB and 1.3 dB was estimated for the ***S***- and ***k***-vector prisms, respectively. Beam steering angles demonstrated here were not so large, since the prisms were optimized for high resolution. It was also shown that the material dispersion near the electronic band-edge can enhance the steering angle. These results strongly encourage future experimental studies. This work was supported by IT Program and 21st COE Program of MEXT, and by CREST of JST.